

# Aura/OMI Above-cloud Aerosol Product-OMACA

## README File

Product Version: 1.4.4

Released Date: Sep 19, 2017

Omar Torres<sup>1</sup> & Hiren Jethva<sup>1,2</sup>

<sup>1</sup>NASA Goddard Space Flight Center, Greenbelt, MD 20771 USA

<sup>1,2</sup>Universities Space Research Association, Columbia, MD 21044 USA

E-mail: [omar.o.torres@nasa.gov](mailto:omar.o.torres@nasa.gov); [hiren.t.jethva@nasa.gov](mailto:hiren.t.jethva@nasa.gov)

## Table of Contents

1. Overview.....	3
2. Algorithm Description – Version 1.4.4 (this release) .....	3
2.1 Physical Basis .....	3
2.2 Inputs and Ancillary Dataset.....	4
2.2.1 UV Aerosol Index (Mie).....	4
2.2.2 Aerosol Layer Height.....	5
2.2.3 Surface Albedo.....	5
2.2.4 Aerosol Type Selection.....	5
2.2.5 Aerosol Single-scattering Albedo above Cloud.....	5
2.2.6 Look-up-tables .....	7
2.2.7 Retrieved Parameters .....	7
2.2.8 Row Anomaly .....	9
3. Data Quality Assessment .....	9
4. Data File Description .....	11
5. History of Algorithm Upgrades .....	13
References.....	14
APPENDIX I .....	15
Sample IDL Reader.....	17

## 1. Overview

The NASA OMI above-cloud aerosols data product, formally named as OMACA, consists of the above-cloud columnar aerosol extinction optical depth (ACAOD) and aerosol-corrected cloud optical depth (COD) at 354 nm, 388 nm, and 500 nm retrieved from the OMACA algorithm. Readers are cautioned here that the OMACA algorithm is different from the standard OMI/OMAERUV aerosol data product. While the OMACA aerosol product reports aerosol optical depth (AOD) above the cloud and only operates on cloudy pixels, the two-channel OMAERUV aerosol algorithm retrieves AOD and single-scattering albedo (SSA) over cloud-free pixels.

This document provides a brief description of the OMI/OMACA Level-2 above-cloud aerosol data products derived from the near-UV observations made by the Ozone Monitoring Instrument (OMI) on the EOS-Aura satellite. The information in this README file applies to **the second public release of the OMACA version 1.4.4 data** of collection 3. As subsequent data versions are produced and released, the README file will be updated accordingly to reflect the latest algorithm modifications and data quality assessments.

The OMACA algorithm physically relies on a strong and unambiguous sensitivity of satellite-based near-UV radiance measurements to the aerosol loading above the cloud and underlying cloud optical properties [Torres *et al.*, 2012]. It employs the top-of-atmosphere (TOA) measurements at 354 nm and 388 nm made by OMI to retrieve the ACAOD and COD at 388 nm. The inversion is made under a set of assumptions about aerosol models (carbonaceous aerosols or dust particles), aerosol layer height, surface albedo, and cloud properties. The retrieved quantities are also reported at 354 nm and 500 nm wavelengths following the spectral dependence of extinction associated with the selected aerosol model. Since the conversion of 388-nm retrieval to the 354 nm and 500 nm is based on the assumed aerosol model, the reported values at these wavelengths should be considered less reliable.

This document is intended to present a brief description of the OMACA algorithm, its various components, and data product.

## 2. Algorithm Description – Version 1.4.4 (this release)

### 2.1 Physical Basis

The presence of absorbing aerosols such as carbonaceous aerosols generated from biomass burning and windblown dust particles above cloud decks reduces the amount of upwelling ultraviolet (UV), visible (VIS), and shortwave infrared radiation reaching the top of atmosphere (TOA). This effect is often referred to as “cloud darkening”, which can be seen by eye in images and quantitatively in the spectral reflectance measurements made by passive sensors such as OMI. The UV Aerosol Index (UV-AI) measured by OMI is an excellent indicator of the presence

of absorbing aerosols in the clear [Torres *et al.*, 1998] as well as cloudy atmosphere [Torres *et al.*, 2012]. The elevated layers of absorbing aerosols when overlay low-level cloud deck produces a strong spectral contrast between the TOA measurements in the two near-UV channel (354 and 388 nm), which enhances the magnitudes of UV-AI. Radiative transfer simulations show that under a set of prescribed atmosphere, the reduction in the spectral reflectance and UV-AI which is quantified using the color ratio information, between a pair of wavelengths is a combined function of both aerosol and cloud optical depths. This forms the physical basis of the simultaneous retrieval of above-cloud aerosol optical depth (ACAOD) and aerosol-corrected cloud optical depth (COD) from OMI observations. Since the technique is physically based on the spectral contrast in the TOA measurements, it is formally named as ‘color ratio’ method. The sensitivity study, technique, and its application to different case studies of carbonaceous aerosols above the cloud over the southeastern Atlantic Ocean are documented in Torres *et al.* [2012].

## 2.2 Inputs and Ancillary Dataset

The OMI Level-1b calibrated and geo-located radiance measurements at 354 and 388 nm are the primary inputs to the OMACA algorithm. In order to retrieve ACAOD and aerosol-corrected COD, OMACA uses a set of the ancillary dataset and assumes specific aerosol models.

### 2.2.1 UV Aerosol Index (Mie)

The UV Aerosol Index or UV-AI is a residual quantity resulting from the comparison between measured and calculated radiances between 354 nm and 388 nm. The calculated radiance was obtained using a simple model of the Earth-atmosphere system consisting of a molecular atmosphere bounded at the bottom by a Lambert Equivalent Reflector (LER) [Dave and Mateer, 1967]. A key assumption in this model representation of the Earth-atmosphere system is that the reflectivity of the column atmosphere’s lower boundary is wavelength independent in the near-UV. The detailed description of the LER-based UV-AI calculations can be found in Herman *et al.* (1997) as well as Torres *et al.* (1998).

Recently, the approach to calculate UV-AI has been revisited. In order to account for the effects of clouds on UV-AI, the new UV-AI is now being calculated using a combination of molecular atmosphere and realistic C1 water cloud model [Deirmendjian, 1969]. The model radiances calculated for the Rayleigh atmosphere and C1 cloud model with cloud optical depth of 10 are used to derive the cloud fraction, which subsequently used to calculate radiances through a linear combination of cloud fraction weighted Rayleigh and cloud radiances. The calculated and observed radiances are then compared to derive UV-AI. Since the new UV-AI is based on the Mie cloud calculation, it is formally called as UV-AI (Mie). A more detailed description on UV-AI (Mie) will be provided in the future publication.

### 2.2.2 Aerosol Layer Height

For the representation of aerosol vertical profile, a climatology database of aerosol layer height (ALH) derived using 30-month long combined and co-located measurements of CALIOP vertical back-scatter and OMI UV-AI is used. The climatology covers most regions of the globe where seasonally varying loads of desert dust and carbonaceous are known to reside. For the radiative transfer calculations required to generate look-up-tables, four discrete aerosol layer heights are considered, i.e., 3, 4, 5, 6 km referenced at surface level (0 km, 4 km). The aerosol profile follows a Gaussian distribution around mean ALH given by the CALIOP-OMI climatology dataset.

### 2.2.3 Surface Albedo

The OMACA uses global, monthly, gridded (0.25-degree x 0.25-degree) near-UV surface albedo database derived from 7-year long (2005-2011) co-located OMI reflectivity or LER observations and MODIS surface reflectance database. The method is essentially based on minimum reflectivity approach. The darkest scene observed by OMI is considered to be free of aerosol and cloud contamination which then temporally adjusted following the temporal pattern of visible surface reflectance retrieved from MODIS. The OMACA algorithm operates on cloudy pixels with measured reflectivity values larger than 0.20 for which the contribution of the surface to the TOA reflectance is expected to be minimum or even negligible for the scenes with opaque clouds.

### 2.2.4 Aerosol Type Selection

Currently, OMACA considers two major absorbing types of aerosols, i.e., carbonaceous smoke aerosols and dust particles. The details of the microphysical and optical properties of the both types of aerosol models are given in APPENDIX I. Aerosol-type identification scheme is adopted from the operational clear-sky OMI/OMAERUV version 1.8.9.1 aerosol product released in September 2017. The scheme uses space and time co-located Aura/OMI UV-AI and Aqua/AIRS Collection 6 columnar retrievals of Carbon Monoxide (CO) to distinguish carbonaceous aerosols and dust particles, which subsequently interpreted to select either smoke or dust model depending upon the magnitude of CO.

### 2.2.5 Aerosol Single-scattering Albedo above Cloud

For the assumption about above-cloud aerosol single-scattering albedo (SSA), we take advantage of the cloud-free standard OMAERUV retrievals of SSA. The whole globe is divided into 14 discrete regions based upon the expected patterns of absorbing aerosols above cloud inferred from the frequency of occurrence analysis. For each region and for each day of observation, the representative value of above-cloud SSA was estimated using the UV-AI weighted clear-sky SSA retrieval (QFlag = 0, best) for all 14 regions. This exercise was carried out for both aerosol types, i.e., carbonaceous aerosols and dust particles over all the regions. Any observation of

aerosols above cloud found outside the boundaries of the pre-selected regions was assigned a fixed value of SSA depending on the selected aerosol type, i.e.,  $SSA=0.8879$  for carbonaceous aerosols and  $SSA=0.90532$  for dust aerosols. Figure 1 shows the time-series of daily regional SSA (388 nm) for different regions.

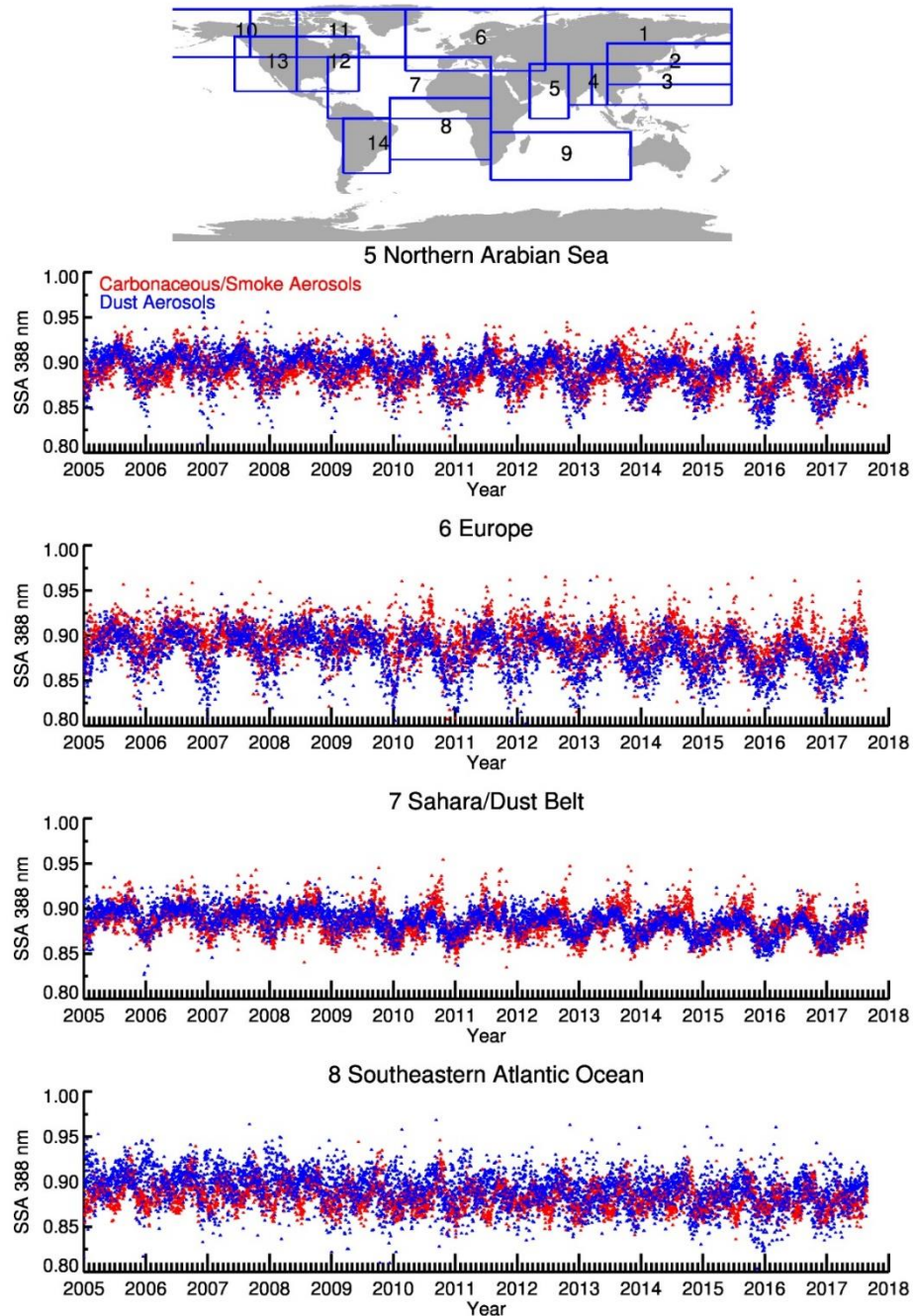


Figure 1 (Top panel) Geographical boundaries of the pre-selected 14 regions. (Rest four panels) Time-series of daily regional SSA (388 nm) calculated for the carbonaceous/smoke aerosols (red) and dust particles (blue) as described in section 2.2.5.

### 2.2.6 Look-up-tables

The OMACA is essentially a look-up-table (LUTs) based algorithm, in which the observations at near-UV wavelengths are matched with the pre-calculated radiances. For generating LUTs, the vector discrete ordinate radiative transfer model VLIDORT [Spurr, 2006] was used. This code offers full linearization ability with outputs of the Stoke vector for arbitrary viewing geometry and the optical thickness of aerosols and cloud. The model results have been compared and benchmarked against the established results in the literature and also used in recent studies of retrieval of ACAOD from space-based sensors [Torres *et al.*, 2012; Jethva *et al.*, 2013; Jethva *et al.*, 2014]. Clouds are assumed to be liquid in phase and follow standard C1 size distribution [Deirmendjian, 1969]. Aerosol size distribution is assumed to follow a bi-modal log-normal distribution with parameters adopted from the standard OMAERUV aerosol models.

LUTs were generated for carbonaceous and dust aerosol models where each aerosol type consists of seven discrete aerosol SSA (388 nm) ranging from 0.75 to 1.00. Carbonaceous aerosols are assumed to be of spherical shape, whereas dust particles The radiative transfer calculations were carried out at the 354- and 388-nm wavelengths and for the seven nodal points in ACAOD (0.0, 0.1, 0.5, 1.0, 2.5, 4.0, and 6.0 at 500 nm) and eight nodal values in COD (0, 2, 5, 10, 20, 30, 40, and 50) at different geometries of solar zenith angle ( $0^\circ, 20^\circ, 40^\circ, 60^\circ, 66^\circ, 72^\circ, 80^\circ$ ), view zenith angle ( $0^\circ, 12^\circ, 18^\circ, 26^\circ, 32^\circ, 36^\circ, 40^\circ, 46^\circ, 50^\circ, 54^\circ, 56^\circ, 60^\circ, 66^\circ, 72^\circ$ ), and relative azimuth angle ( $0^\circ$ - $150^\circ$  in step of  $30^\circ$ , and  $160^\circ, 165^\circ, 170^\circ, 175^\circ, 180^\circ$ ). The simulations were carried out for the two surface pressure levels (1013.25 hPa, 800 hPa) and assuming four different ALH, i.e., 3, 4, 5, 6 km referenced at respective surface pressure levels.

### 2.2.7 Retrieved Parameters

The LUT radiances interpolated at observed geometry, pressure level, aerosol layer height, and single-scattering albedo are matched with the OMI-observed radiance in 2D retrieval domain (UV-AI versus radiance at 388 nm), as shown in Figure 2, in order to find a pair of ACAOD and COD at 388 nm. The retrieved values at 388 nm were converted to 354 nm and 500 nm wavelengths based on the spectral dependence of extinction associated with the assumed model.

Figure 3 illustrates the flowchart of the OMACA algorithm.

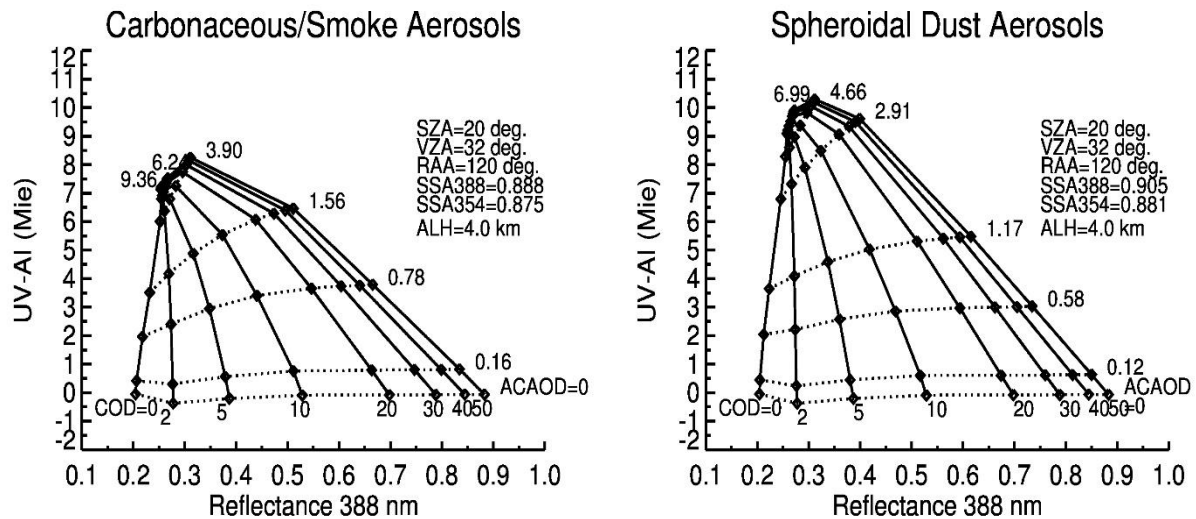


Figure 2 Simulation of UV-AI (y-axis) versus Reflectance at 388 nm (x-axis) for the different pairs of ACAOD and COD (both at 388 nm) for the carbonaceous (left) and spheroidal dust aerosols (right). Values of ACAOD and COD depicted in the figure correspond to 3388 nm. The shown 2-D diagram forms the retrieval domain in which the observations from OMI are fitted and related to a pair of ACAOD and COD.

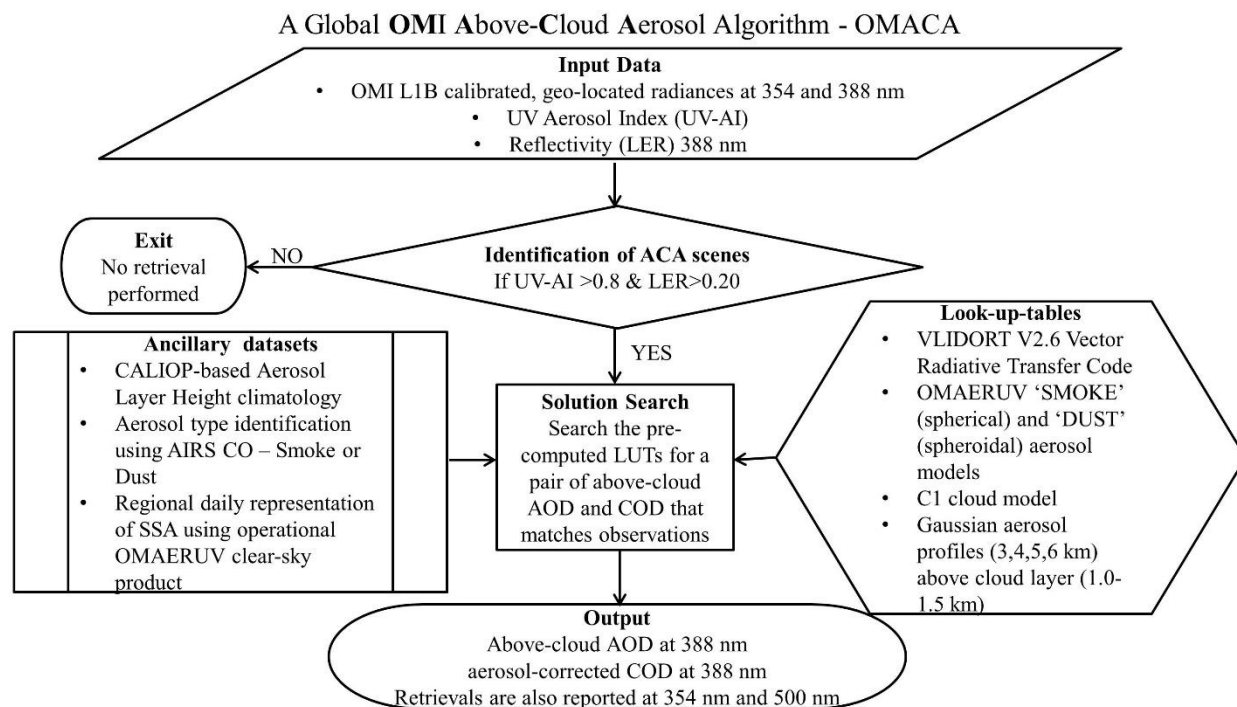


Figure 3 Flow chart of the global OMACA algorithm.

### 2.2.8 Row Anomaly

Since mid-2007, OMI observations have been affected by a likely external obstruction that perturbs both the measured solar flux and Earth radiance. This obstruction affecting the quality of radiance at all wavelengths for a particular viewing direction is referred to as “row anomaly” since the viewing geometry is associated with the row numbers on the charge-coupled device detectors. The row anomaly issue was detected first time in mid-2007 with a couple of rows which over the period of operation expanded to other rows in 2008 and later. At present, about half of the total 60 rows across the track are identified and flagged as row anomaly affected positions for which no physical retrievals from all standard operational OMI algorithms, including OMACA, are being performed.

The screening of row anomaly data in OMACA has been carried out using *XtrackQualityFlags* field reported in the OMI L1B swath file. The *XtrackQualityFlags* field has been added to the Geolocation Fields of Level-2 file. The information of bit values for this field is available at the website <http://www.knmi.nl/omi/research/product/rowanomaly-background.php>.

It is possible to find additional row anomalies not fully characterized in the data so that care must be taken in using data since 2009. A further improved flagging scheme is an ongoing development and will be updated periodically as new anomaly develops.

## 3. Data Quality Assessment

OMACA has adopted a simplified algorithm flag scheme which assigns each pixel with valid ACAOD retrieval a flag that describes the quality of the retrieval. While pixels with larger magnitudes of UV-AI and LER388 are expected to be the best retrieval (*FinalAlgorithmFlags* = 0), retrievals with lower magnitudes of both parameters might be of inferior quality (*FinalAlgorithmFlags* = 1, 2) due to less confidence in the detection of either overcast pixels (lower LER388) or the presence of absorbing aerosols above cloud (lower UV-AI). Retrievals with *FinalAlgorithmFlags* equals 3 should not be used in any scientific analysis as this data has been derived using the observations made at the extreme geometry conditions which produce a false aerosol signal and thus spurious UV-AI for cloudy pixels. Data with *FinalAlgorithmFlags* 4 to 8 are devoid of any retrieval due to either snow/ice contamination (4), solar zenith angle exceedance above the threshold value of 70 degree (5), terrain pressure below the threshold of 800 hPa (7), and cross track row anomaly (8). Table 1 describes algorithm quality flags assigned to each valid retrieval.

Table 1 OMACA Algorithm Quality Flags

Algorithm Quality Flags	Observation Conditions	Description
0	UV-AI (Mie) >1.3 & LER <sub>388</sub> >0.25	Best quality retrievals
1	1.3<UV-AI (Mie) <4.3& 0.20<LER <sub>388</sub> <0.25	Less confidence on the detection of total overcast pixels (Use of high-res sensors is recommended)
2	0.8<UV-AI (Mie) <1.3 & LER>0.25	Less confidence on the detection of aerosols above cloud
3	Solar Zenith Angle> 55° & Scattering Angle <100° & UV-AI (Mie) <2  Solar Zenith Angle> 60° & Scattering Angle <130° & UV-AI (Mie) <2  Viewing Zenith Angle>55° & Scattering Angle <100° & UV-AI (Mie) <2	Geometry-related artifacts
4	Snow/Ice Contamination	No retrieval
5	Solar Zenith Angle above threshold (70 degrees)	No retrieval
7	Terrain Pressure below threshold (800 hPa).	No Retrieval
8	Cross-track anomaly	No retrieval

Unlike the validation of cloud-free aerosol retrievals from satellites, for which ample ground-based measurements are available, validation of ACAOD is a challenging task primarily due to the lack of adequate direct measurements of aerosols in cloudy skies, specifically of aerosols above the cloud. While ground-based measurements cannot be helpful in this situation, airborne measurements taken when the aircraft is flying above cloud seem to be the only source to validate the above-cloud aerosol retrievals.

NASA's ORACLES-ObseRvations of Aerosols above CLOUDs and their intEractionS (<https://espo.nasa.gov/oracles>) is an ongoing multi-year field experiment funded by the NASA Earth-Venture Suborbital Program. Began in August 2016, the ORACLES experiment intends to make detailed and accurate airborne remote sensing and in situ measurements of the key parameters that govern the cloud-aerosol interaction in the southeastern Atlantic Ocean. Owing to the huge abundance of lofted biomass burning aerosols over the semi-permanent marine boundary layer stratocumulus cloud deck, this region serves as a perfect natural laboratory to

assess aerosol-cloud-radiation interactions. Note that this is an area with some of the largest inter-model differences in aerosol forcing assessments on the planet. The experiment will employ a suite of sensors including 4STAR and High Spectral Resolution Lidar (HSRL-2) on NASA's P-3B and ER-2 aircrafts, respectively. Both instruments are capable of making measurements of AOD above the cloud and therefore relevant to the assessment of the equivalent satellite retrieval.

In parallel with ORACLES, the Cloud Aerosol Radiation Interactions and Forcing: Year 2016 (CLARIFY-2016) campaign with project partners from the UK Met Office and universities will also take place over the same region with a deployment of airborne and surface-based instruments in conjunction with satellite observations of aerosols and clouds. Both of these planned high-profile experiments will deliver a wide range of direct and in situ observations of aerosol above clouds to provide a better process-level understanding of aerosol-cloud-radiation interactions over the SE Atlantic. Among the planned measurements, direct AOD and detailed optical and microphysical measurements of aerosols above cloud will be germane for validating and improving satellite-based retrievals. Observations from ORACLES and CLARIFY-2016 will challenge and improve the assumptions made in the inversion for achieving better accuracy and reliability.

#### 4. Data File Description

Like all other standard OMI products, the OMACA product is written in HDF-EOS5 swath file format. Each Level-2 orbital data file present data for that particular orbit of OMI. For tools to read HDF-EOS5 data files, please visit the link: <http://disc.gsfc.nasa.gov/Aura/tools.shtml>.

Figure 4 shows a snapshot of the HDFView software showing all the Scientific Datasets stored in a single OMACA L2 orbital data file. As described in the previous section, each valid ACAOD retrieval pixel carries an algorithm quality flag, named as “*FinalAlgorithmFlags*”, which tells the users about the overall data quality of the retrieval. Most users should use data with quality flag 0 as these data represent pixels having higher values of UV-AI (Mie) and LER388-both measurements show an unambiguous signal of absorbing aerosols above the cloud and thus treated as “best” retrievals. Data with quality flag 1 and 2 represent retrieval with lower values in either measurements and thus reduces the confidence in the detection of either fully overcast pixel and/or absorbing aerosols above the cloud. In such situation, users are recommended to use high-resolution measurements from sensors such as MODIS to ensure that the OMI pixel is fully overcast.

Questions and comments related to the OMACA algorithm and product should be directed to Omar Torres (Principal Investigator, [omar.o.torres@nasa.gov](mailto:omar.o.torres@nasa.gov)) and/or Hiren Jethva ([hiren.t.jethva@nasa.gov](mailto:hiren.t.jethva@nasa.gov)). Users are encouraged to contact the NASA OMI aerosol group for the use and interpretation of their results.

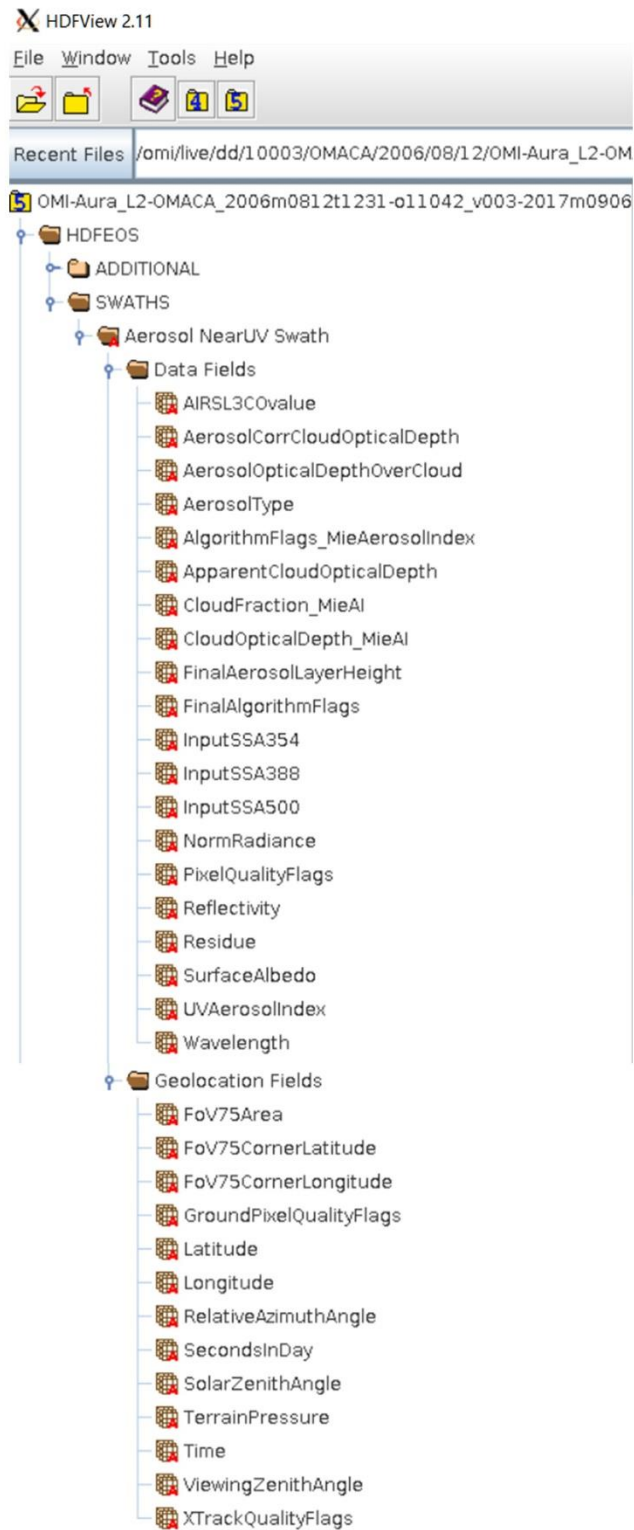


Figure 2 OMACA product SDS as displayed in HDFView software.

Currently, the entire OMI mission record (Oct 1, 2004 to Sep 19, 2017) of OMACA product has been made freely available on the Aura Validation Data Center web portal at the link: <http://avdc.gsfc.nasa.gov/pub/data/satellite/Aura/OMI/V03/L2/OMACA/>. Also, the OMACA algorithm is being run in the forward processing stream with a maximum latency of three days and the AVDC portal is continuously updated with the latest data as they are processed.

## **5. History of Algorithm Upgrades**

The v1.4.4 of OMACA algorithm described briefly in this document is the second version made available to the public. It replaces the first version of the algorithm (v1.0.9) published in July 2016. In between the two public versions, several upgrades were applied to OMACA internally in order to arrive at this version. In the case of further upgrades of OMACA in near future, a new README file will be released with additional information.

## References

- Dave, J.V., and C.L. Mateer (1967), A preliminary study on the possibility of estimating total atmospheric ozone from satellite measurements, *J. Atmos. Sci.*, 24, 414-427
- Deirmendjian, D.: (1969) Electromagnetic Scattering on Spherical Polydispersions, American Elsevier Publishing Company, Inc., New York.
- Herman, J. R., P. K. Bhartia, O. Torres, et al. (1997), Global distribution of UV-absorbing aerosols from Nimbus-7/TOMS data, *J. Geophys. Res.*, 102, 16911-16921.
- Jethva, H., O. Torres, L. A. Remer, and P. K. Bhartia (2013), A color ratio method for simultaneous retrieval of aerosol and cloud optical thickness of above-cloud absorbing aerosols from passive sensors: Application to MODIS measurements, *Geoscience and Remote Sensing, IEEE Transactions on*, 51(7), pp. 3862-3870, doi:10.1109/TGRS.2012.2230008.
- Jethva, H., O. Torres, F. Waquet, D. Chand, and Y. Hu (2014), How do A-train sensors intercompare in the retrieval of above-cloud aerosol optical depth? A case study-based assessment, *Geophys. Res. Lett.*, 41, 186–192, doi:10.1002/2013GL058405.
- Hiren Jethva, Omar Torres and Changwoo Ahn (2016), A ten-year global record of absorbing aerosols above clouds from OMI's near-UV observations, Proc. SPIE 9876, Remote Sensing of the Atmosphere, Clouds, and Precipitation VI, 98761A (May 5, 2016); doi:10.1117/12.2225765; <http://dx.doi.org/10.1117/12.2225765>
- Spurr, R. J. D. (2006), A linearized pseudo-spherical vector discrete ordinate radiative transfer code for forward model and retrieval studies in multilayer multiple scattering media, *J. Quant. Spectrosc. Radiat. Transf.*, 102 (2), pp. 316-342.
- Torres, O., P. K. Bhartia, J. R. Herman, Z. Ahmad, and J. Gleason, (1998), Derivation of aerosol properties from satellite measurements of backscattered ultraviolet radiation: Theoretical basis, *J. Geophys. Res.*, 103(D14), 17,099-17,110 doi:10.1029/98JD00900.
- Torres, O., H. Jethva, and P. K. Bhartia (2012), Retrieval of aerosol optical depth above clouds from OMI observations: Sensitivity analysis and case studies, *J. Atmos. Sci.*, vol. 69, pp. 1037-1053, <http://dx.doi.org/10.1175/JAS-D-11-0130.1>.
- Torres, O., C. Ahn, and Z. Chen, (2013), Improvements to the OMI near-UV aerosol algorithm using A-train CALIOP and AIRS observations, *Atmos. Meas. Tech.*, 6, 3257-3270, doi:10.5194/amt-6-3257-2013.

## APPENDIX I

### OMI/OMACA Carbonaceous Aerosol Models

#### Optical Properties

Model →	1	2	3	4	5	6	7
<b>Imaginary Index</b> 354 /388	0.000 /0.000	0.006 /0.005	0.012 /0.010	0.024 /0.020	0.036 /0.030	0.048 /0.040	0.0576 /0.0480
<b>Single-scattering Albedo</b> 354 /388	1.0 /1.0	0.9602 /0.9644	0.9288 /0.9361	0.8751 /0.8878	0.8287 /0.8458	0.7873 /0.8080	0.7575 /0.7804

Real refractive index 1.50 (wavelength independent)

#### Microphysical Properties

##### For Model 1 to 3

Mean radius/Standard Deviation Fine mode : 0.08717/1.537  $\mu\text{m}$

Mean radius/Standard Deviation Coarse mode : 0.567194/2.203  $\mu\text{m}$

##### For Model 4 to 7

Mean radius/Standard Deviation Fine mode : 0.080132/1.492  $\mu\text{m}$

Mean radius/Standard Deviation Coarse mode : 0.705495/2.075  $\mu\text{m}$

## OMI/OMACA Dust Aerosol Models

### Optical Properties

<b>Model →</b>	<b>1</b>	<b>2</b>	<b>3</b>	<b>4</b>	<b>5</b>	<b>6</b>	<b>7</b>
<b>Imaginary Index 354 /388</b>	0.0/0.0	0.00128 /0.00092	0.00256 /0.00185	0.00561 /0.00405	0.00832 /0.00600	0.01279 /0.00923	0.02303 /0.01622
<b>Single-scattering Albedo 354 /388</b>	1.0/1.0	0.9625 /0.9723	0.9324 /0.9484	0.8779 /0.9023	0.8422 /0.8698	0.7989 /0.8277	0.7370 /0.7635

Real refractive index 1.55 (wavelength independent)

### Microphysical Properties

For all seven aerosol models

Mean radius/Standard Deviation Fine mode : 0.052/1.697  $\mu\text{m}$

Mean radius/Standard Deviation Coarse mode : 0.67/1.806  $\mu\text{m}$

## Sample IDL Reader

;This IDL script reads the OMI/OMACA Level-2 HDF-EOS5 data file. It reads each SDS parameter stored in the HE5 file and returns the respective data in an array format.

```
Filename = '/omi/live/dd/70003/OMACA/2007/08/05/OMI-Aura_L2-OMACA_2007m0805t1155-  
o16255_v003-2016m0530t194355.he5'
```

```
FILE_ID=H5F_OPEN(Filename)
```

```
;Geolocation Data Fields
```

```
;Latitude
```

```
lat_name='/HDFEOS/SWATHS/Aerosol NearUV Swath/Geolocation Fields/Latitude'  
lat_id=H5D_OPEN(FILE_ID,lat_name)  
lat=H5D_READ(lat_id)
```

```
;Dimension of Latitude
```

```
sz=SIZE(lat)  
n=N_ELEMENTS(sz)  
dim=sz(0)  
row=sz(1)  
col=sz(2)
```

```
;Longitude
```

```
lon_name='/HDFEOS/SWATHS/Aerosol NearUV Swath/Geolocation Fields/Longitude'  
lon_id=H5D_OPEN(FILE_ID,lon_name)  
lon=H5D_READ(lon_id)
```

```
;RelativeAzimuthAngle
```

```
phi_name='/HDFEOS/SWATHS/Aerosol NearUV Swath/Geolocation  
Fields/RelativeAzimuthAngle'  
phi_id=H5D_OPEN(FILE_ID,phi_name)  
phi=H5D_READ(phi_id)
```

```
;SecondsInDay
```

```
secs_name='/HDFEOS/SWATHS/Aerosol NearUV Swath/Geolocation Fields/SecondsInDay'  
secs_id=H5D_OPEN(FILE_ID,secs_name)  
secs=H5D_READ(secs_id)
```

```
;SolarZenithAngle
```

```
sza_name='/HDFEOS/SWATHS/Aerosol NearUV Swath/Geolocation Fields/SolarZenithAngle'  
sza_id=H5D_OPEN(FILE_ID,sza_name)  
sza=H5D_READ(sza_id)
```

```
;TerrainPressure
```

```
tpres_name='/HDFEOS/SWATHS/Aerosol NearUV Swath/Geolocation Fields/TerrainPressure'  
tpres_id=H5D_OPEN(FILE_ID,tpres_name)
```

```
tpres=H5D_READ(tpres_id)

;Time
time_name='/HDFEOS/SWATHS/Aerosol NearUV Swath/Geolocation Fields/Time'
time_id=H5D_OPEN(FILE_ID,time_name)
time=H5D_READ(time_id)

;ViewingZenithAngle
vza_name='/HDFEOS/SWATHS/Aerosol NearUV Swath/Geolocation Fields/ViewingZenithAngle'
vza_id=H5D_OPEN(FILE_ID,vza_name)
vza=H5D_READ(vza_id)

;RelativeAzimuthAngle
phi_name='/HDFEOS/SWATHS/Aerosol NearUV Swath/Geolocation
Fields/RelativeAzimuthAngle'
phi_id=H5D_OPEN(FILE_ID,phi_name)
phi=H5D_READ(phi_id)

;*****
;DATA FILEDS

;AerosolCorrCloudOpticalDepth
cod_name='/HDFEOS/SWATHS/Aerosol NearUV Swath/Data
Fields/AerosolCorrCloudOpticalDepth'
cod_id=H5D_OPEN(FILE_ID,cod_name)
cod=H5D_READ(cod_id)

cod354=FLTARR(row,col)
cod388=FLTARR(row,col)
cod500=FLTARR(row,col)

cod354(*,*)=cod(0,*,*) ;COD at 354 nm
cod388(*,*)=cod(1,*,*) ;COD at 388 nm
cod500(*,*)=cod(2,*,*) ;COD at 500 nm

;AerosolOpticalDepthOverCloud
acaod_name='/HDFEOS/SWATHS/Aerosol NearUV Swath/Data
Fields/AerosolOpticalDepthOverCloud'
acaod_id=H5D_OPEN(FILE_ID,acaod_name)
acaod=H5D_READ(acaod_id)

acaod354=FLTARR(row,col)
acaod388=FLTARR(row,col)
acaod500=FLTARR(row,col)

acaod354(*,*)=acaod(0,*,*) ;Above-cloud AOD at 354 nm
acaod388(*,*)=acaod(1,*,*) ;Above-cloud AOD at 388 nm
acaod500(*,*)=acaod(2,*,*) ;Above-cloud AOD at 500 nm
```

```
;AerosolType
aertype_name='/HDFEOS/SWATHS/Aerosol NearUV Swath/Data Fields/AerosolType'
aertype_id=H5D_OPEN(FILE_ID,aertype_name)
aertype=H5D_READ(aertype_id)
```

```
;AlgorithmFlags_MieAerosolIndex
algflags_MieAI_name='/HDFEOS/SWATHS/Aerosol NearUV Swath/Data
Fields/AlgorithmFlags_MieAerosolIndex'
algflags_MieAI_id=H5D_OPEN(FILE_ID,algflags_MieAI_name)
algflags_MieAI=H5D_READ(algflags_MieAI_id)
```

```
;ApparentCloudOpticalDepth
appcod_name='/HDFEOS/SWATHS/Aerosol NearUV Swath/Data
Fields/ApparentCloudOpticalDepth'
appcod_id=H5D_OPEN(FILE_ID,appcod_name)
appcod=H5D_READ(appcod_id)
```

```
appcod354=FLTARR(row,col)
appcod388=FLTARR(row,col)
appcod500=FLTARR(row,col)
```

```
appcod354(*,*)=appcod(0,*,*) ;APPCOD at 354 nm
appcod388(*,*)=appcod(1,*,*) ;APPCOD at 388 nm
appcod500(*,*)=appcod(2,*,*) ;APPCOD at 500 nm
```

```
;InputSSA388
ssa388_name='/HDFEOS/SWATHS/Aerosol NearUV Swath/Data Fields/InputSSA388'
ssa388_id=H5D_OPEN(FILE_ID,ssa388_name)
ssa388=H5D_READ(ssa388_id)
```

```
;InputSSA354
ssa354_name='/HDFEOS/SWATHS/Aerosol NearUV Swath/Data Fields/InputSSA354'
ssa354_id=H5D_OPEN(FILE_ID,ssa354_name)
ssa354=H5D_READ(ssa354_id)
```

```
;CloudFraction_MieAI
cldfrac_MieAI_name='/HDFEOS/SWATHS/Aerosol NearUV Swath/Data
Fields/CloudFraction_MieAI'
cldfrac_MieAI_id=H5D_OPEN(FILE_ID,cldfrac_MieAI_name)
cldfrac_MieAI=H5D_READ(cldfrac_MieAI_id)
```

```
;CloudOpticalDepth_MieAI
cod_MieAI_name='/HDFEOS/SWATHS/Aerosol NearUV Swath/Data
Fields/CloudOpticalDepth_MieAI'
cod_MieAI_id=H5D_OPEN(FILE_ID,cod_MieAI_name)
cod_MieAI=H5D_READ(cod_MieAI_id)
```

```
;FinalAerosolLayerHeight
finalh_name='/HDFEOS/SWATHS/Aerosol NearUV Swath/Data Fields/FinalAerosolLayerHeight'
finalh_id=H5D_OPEN(FILE_ID,finalh_name)
finalh=H5D_READ(finalh_id)

;FinalAlgorithmFlags
finalgflags_name='/HDFEOS/SWATHS/Aerosol NearUV Swath/Data
Fields/FinalAlgorithmFlags'
finalgflags_id=H5D_OPEN(FILE_ID,finalgflags_name)
finalgflags=H5D_READ(finalgflags_id)

;NormalizedRadiance
normrad_name='/HDFEOS/SWATHS/Aerosol NearUV Swath/Data Fields/NormRadiance'
normrad_id=H5D_OPEN(FILE_ID,normrad_name)
normrad=H5D_READ(normrad_id)

normrad354=FLTARR(row,col)
normrad388=FLTARR(row,col)
normrad500=FLTARR(row,col)

normrad354(*,*)=normrad(0,*,*)      ;Normalized Radiance at 354 nm
normrad388(*,*)=normrad(1,*,*)      ;Normalized Radiance at 388 nm
normrad500(*,*)=normrad(2,*,*)      ;Normalized Radiance at 500 nm

;Reflectivity
ler_name='/HDFEOS/SWATHS/Aerosol NearUV Swath/Data Fields/Reflectivity'
ler_id=H5D_OPEN(FILE_ID,ler_name)
ler=H5D_READ(ler_id)

ler354=FLTARR(row,col)
ler388=FLTARR(row,col)
ler500=FLTARR(row,col)

ler354(*,*)=ler(0,*,*)      ;Reflectivity at 354 nm
ler388(*,*)=ler(1,*,*)      ;Reflectivity at 388 nm
ler500(*,*)=ler(2,*,*)      ;Reflectivity at 500 nm

;SurfaceAlbedo
surfalb_name='/HDFEOS/SWATHS/Aerosol NearUV Swath/Data Fields/SurfaceAlbedo'
surfalb_id=H5D_OPEN(FILE_ID,surfalb_name)
surfalb=H5D_READ(surfalb_id)

surfalb354=FLTARR(row,col)
surfalb388=FLTARR(row,col)
surfalb500=FLTARR(row,col)

surfalb354(*,*)=surfalb(0,*,*)      ;SurfaceAlbedo at 354 nm
surfalb388(*,*)=surfalb(1,*,*)      ;SurfaceAlbedo at 388 nm
surfalb500(*,*)=surfalb(2,*,*)      ;SurfaceAlbedo at 500 nm

;UVAerosolIndex
uvai_name='/HDFEOS/SWATHS/Aerosol NearUV Swath/Data Fields/UVAerosolIndex'
```

```
uvai_id=H5D_OPEN(FILE_ID,uvai_name)
uvai=H5D_READ(uvai_id)
```

```
H5D_CLOSE,lat_id
H5D_CLOSE,lon_id
H5D_CLOSE,phi_id
H5D_CLOSE,secs_id
H5D_CLOSE,sza_id
H5D_CLOSE,tpres_id
H5D_CLOSE,time_id
H5D_CLOSE,vza_id
```

```
H5D_CLOSE,cod_id
H5D_CLOSE,acaod_id
H5D_CLOSE,aertype_id
H5D_CLOSE,algflags_MieAI_id
H5D_CLOSE,appcod_id
H5D_CLOSE,ssa354_id
H5D_CLOSE,ssa388_id
H5D_CLOSE,cldfrac_MieAI_id
H5D_CLOSE,cod_MieAI_id
H5D_CLOSE,finalh_id
H5D_CLOSE,finalgflags_id
H5D_CLOSE,normrad_id
H5D_CLOSE,ler_id
H5D_CLOSE,surfalb_id
H5D_CLOSE,uvai_id
```

```
H5F_CLOSE,FILE_ID
```

```
END ;End of procedure
```